Published in final edited form as:
Brain Res. 2009 June 18; 1276: 67–76. doi:10.1016/j.brainres.2009.04.025.

Development and Aging of the Healthy Human Brain Uncinate Fasciculus across the Lifespan using Diffusion Tensor Tractography

Khader M. Hasan[1], **Amal Iftikhar**[1], **Arash Kamali**[1], **Larry A. Kramer**[1], **Manzar Ashtari**[5], **Paul T. Cirino**[3,4], **Andrew C. Papanicolaou**[2], **Jack M. Fletcher**[3], and **Linda Ewing-Cobbs**[2]

1 *Department of Diagnostic and Interventional Imaging, University of Texas Health Science Center at Houston-Medical School*

2 *Department of Pediatrics, University of Texas Health Science Center at Houston-Medical School*

3 *Department of Psychology, University of Houston*

4 *Texas Institute for Measurement, Evaluation, and Statistics Houston, Texas*

5 *Department of Radiology, The Children's Hospital of Philadelphia, Philadelphia, PA 19104*

Abstract

The human brain uncinate fasciculus (UF) is an important cortico-cortical white matter pathway that directly connects the frontal and temporal lobes, although there is a lack of conclusive support for its exact functional role. Using diffusion tensor tractography, we extracted the UF, calculated its volume and normalized it with respect to each subject's intracranial volume (ICV) and analyzed its corresponding DTI metrics bilaterally on a cohort of 108 right-handed children and adults aged 7–68 years. Results showed *inverted* U-shaped curves for fractional anisotropy (FA) with advancing age and U-shaped curves for radial and axial diffusivities reflecting white matter progressive and regressive myelination and coherence dynamics that continue into young adulthood. The mean FA values of the UF were significantly larger on the left side in children ($p=0.05$), adults ($p=0.0012$) and the entire sample ($p=0.0002$). The FA leftward asymmetry (Left > Right) is shown to be due to increased leftward asymmetry in the axial diffusivity ($p<0.0001$) and a lack of asymmetry ($p>0.23$) for the radial diffusivity. This is the first study to provide baseline normative macro and microstructural age trajectories of the human UF across the lifespan. Results of this study may lend themselves to better understanding of UF role in future behavioral and clinical studies.

Keywords

Diffusion tensor imaging; fiber tracking; uncinate fasciculus; child; adult; brain development; aging; lifespan

*Corresponding Author: Khader M. Hasan, Ph.D., Associate Professor of Diagnostic and Interventional Imaging, Department of Diagnostic and Interventional Imaging, University of Texas Medical School at Houston, 6431 Fannin Street, MSB 2.100, Houston, Texas 77030, Tel: Office (713) 500-7690, Fax: (713) 500-7684, Email: E-mail: Khader.M.Hasan@uth.tmc.edu.

1. Introduction

The human uncinate fasciculus (small hook-shaped bundle) connects the inferior frontal gyrus and the inferior surfaces of the frontal lobe with the anterior portions of the temporal lobe (Ebeling and Cramon, 1992; Kier et al., 2004; Schmahmann and Pandya, 2006). The exact role of the UF's function and its relevant human behavioral relations are not yet resolved (Catani and Mesulam, 2008; Duffau et al., 2009; Parker et al., 2005). The UF is traditionally considered to be part of the limbic system and is known for its involvment in human emotion processing, memory and language functions (Schmahmann et al., 2008).

To the best of our knowledge, Highley et al. (2002) is the only postmortem histological study on the human UF that reported a rightward asymmetry of the area and fiber density for this structure in older adults. The UF has been used as a marker of tissue integrity in noninvasive magnetic resonance imaging (MRI) studies in healthy (Catani et al., 2002; Mamata et al., 2002) and diseased (Antunes et al., 2002; Aralasmak et al., 2006; Borroni et al., 2008; Kier et al., 2004; Kezele et al., 2008; Hasan et al., 2009b) populations. Other DTI reports on the UF includes using region-of-interest (Kubicki et al., 2002), voxel-based (Burns. et al., 2003; Park et al., 2004), and fiber tracking deterministic approaches (Catani et al., 2002; Mori et al., 2002) and probabilistic methods (Hagmann et al., 2003) to clarify changes related to tissue maturation (Dubois et al., 2006), development (Constable et al., 2008; Eluvathingal et al., 2007; Lebel et al., 2008) and normal aging (Zahr et al., 2009). The UF has also been studied using DTI methods in several clinical conditions that include frontotemporal dementia (Fujie et al., 2008; Matsu et al., 2008), Alzheimer's (Taoka et al., 2006), mental retardation (Yu et al., 2008), social deprivation (Eluvathingal et al., 2006), depression (Sheline et al., 2008), bipolar disorder (Houenou et al., 2008), schizophrenia (Nakamura et al., 2005; Kanaan et al., 2005; Price et al., 2008; Szeszko et al., 2008), spina bifida (Hasan et al., 2008), traumatic brain injury (Niogi et al., 2008), temporal lobe epilepsy (Diehl et al., 2008; Rodrigo et al., 2007; Mcdonald et al., 2008) and multiple sclerosis as a marker of Wallerian degeneration (Hasan et al., 2009b).

In general, there is limited literature on the normal aging trajectories and normative values for UF macro (morphometry) and micro-structures (morphology) (Schmahmann and Pandya, 2006). Age has been shown to be a confounding factor in the interpretation of clinical data from structures such as the UF (Jones et al., 2006). Due to differences in acquisition and analysis methods between studies with relatively small population size, the available DTI reports (see Table 1) have provided a conflicting and incomplete account of the UF age, gender and diffusion anisotropy asymmetry in both children and adults. To our knowledge, there has been no cross-sectional quantitative MRI study on healthy controls across the lifespan for evaluation of the UF macrostructural (e.g. volume) and microstructure (e.g. diffusion indices).

In this work, we applied DTI fiber tracking methods as described previously (Eluvathingal et al., 2007) on a cohort of right-handed children and adults to quantify the spatiotemporal trajectories of the UF volumes bilaterally along with its corresponding DTI indices such as fractional anisotropy, radial and axial diffusivities. Given previous DTI works on whole brain white matter (Hasan et al., 2007b) and regional white matter tracking trends (Hasan et al., 2009a) that identified nonlinear relationships of DTI metrics with age, we hypothesized that the microstructural attributes of the UF development and aging trajectories would be best characterized by nonlinear curves across the human lifespan.

2. Results

2.1 Uncinate Fasciculus Absolute and Normalized Volume: Group Differences and Sex Effects

Group mean values and comparisons of the intracranial volume (ICV) and the right and left UF volume (UFV) on all possible subgroups of study participants (boys, girls, men, women, children and adults) are summarized in Table 2. The ICV was not significantly different between boys and men ($p = 0.27$). The ICV was not significantly different between girls and women ($p=0.08$). The ICV was significantly larger in males compared to females ($p<0.000001$; see Table 2). The ICV and right UFV were larger in males compared to females ($p<0.005$). The UF volume-to-ICV ratios (UFV/ICV × 100%) were not significantly different between males and females ($p>0.14$).

2.2 Uncinate Fasciculus DTI Metrics: Group Differences and Sex Effects

The UF corresponding FA, radial and axial diffusivity are summarized in Table 3. There were no significant differences between males and females ($p>0.14$; see Table 3). Therefore, age effect results are from a pooled sample of males and females.

2.3 Age Effects

Pearson correlation coefficients of the UFV/ICV, FA, radial and axial diffusivities and age for all children and adults are summarized in Table 4. Note the lack of dependence on age in the normalized UFV between children ($p>0.2$) and adults ($p>0.13$). The DTI metrics in Table 4 show that children have significant linear trends compared to adults which necessitated quadratic least-squares modeling for the age effects. Table 5 summarizes the least-squares coefficients using the quadratic least-squares (QLS) model, standard deviation and significance. The scatter data, least and quadratic least-squares fits of the normalized UF volume, corresponding FA, radial and axial diffusivity are plotted in Figure 1 and Figure 2 for both the right and left UF respectively.

2.4 Asymmetry effects

There were no statistically significant age-by-sex or age-by-hemisphere interactions. Comparison of linear and quadratic coefficients for both males and females showed no differences between males and females ($p>0.3$). The absolute and ICV-normalized UF volumes for the right side were larger as compared with the left in children ($p=0.02$) but not significantly different either in adults ($p>0.56$) or in the entire population ($p=0.27$). The mean FA values of the UF were significantly larger on the left side in children ($p=0.05$), adults ($p=0.0012$) and the entire sample ($p=0.0002$). This leftward asymmetry (Left > Right) in the diffusion anisotropy is explained by a leftward asymmetry in the axial diffusivity ($p<0.0001$) and a lack of asymmetry ($p>0.23$) in the radial diffusivity.

3. Discussion

The UF has been used as a marker of development, natural aging and disconnection of the temporal and frontal lobes that result from surgical interventions (Kier et al., 2004; Wurm et al., 2000; Schoene-Bake et al., 2009), congenital (Hasan et al., 2008), traumatic (Levine et al., 1998), and degenerative disorders (Aralasmak et al., 2006; Kanaan et al., 2005; Hasan et al., 2009b). Quantitative noninvasive MRI literature on the UF *across the human lifespan* is generally scant. To the best of our knowledge, this is the first cross-sectional lifespan study on the development and aging of the UF in both hemispheres using DTI fiber tracking methods. We have presented and compared both absolute UF volumes and ICV-normalized values to reduce effects related to human brain size variability (Im et al. 2008; Walhovd et al., 2005).

The ICV values in our healthy cohort are comparable to those reported in other studies in controls (Buckner et al., 2004). The fiber-tracked UF volume and its ICV-normalized values exhibited larger variability compared with the corresponding DTI metrics. Large variability in fiber tract volume using DTI has also been reported on the cingulum (Heiervang et al., 2007), the corticospinal tract (Reich et al., 2006), and uncinate fasciculus (Wakana et al., 2007). To the best of our knowledge, only three DTI publications documented the UF volume and its corresponding DTI metrics on healthy adults (Malykhin et al., 2009; Taoka et al., 2006; Wakana et al., 2007; see Table 1). Some studies on the UF using coronal 2D ROIs may have included the inferior fronto-occipital fasciculus (Catani et al., 2002; see Kanaan et al., 2005 for details).

The volume measurements of the UF in our adult population (see Table 2) are larger than those reported previously (Malykhin et al., 2009; Taoka et al., 2006;Wakana et al., 2007) in adult controls (see Table 1). These differences may be attributed to differences between samples used (e.g. age, brain size), DTI acquisition paradigm (e.g. voxel size, signal-to-noise ratio) and analysis procedures (e.g. tracking thresholds). Consistent with previous reports in the healthy UF (see Table 1), we report no sex differences on the normalized UF and its corresponding DTI metrics.

3.1 Age and Sex Effects

Our DTI results on the development and aging of the UF consolidate previous normative studies (see Table 1) that reported positive linear age trends in healthy children (Eluvathingal et al., 2007) and young adults (Lebel et al., 2008), and negative age trends in older adults (Jones et al., 2006). The current work UF DTI age trajectories resemble those published on whole brain white matter (Hasan et al., 2007b), lobar (Sowell et al., 2003) and subcortical volumes (e.g. hippocampus and amygdala see Walhovd et al., 2005).

The DTI-related metrics (FA, eigenvalues) provide complementary information about the microstructural substrates of tissue organization (Beaulieu, 2002; Hasan et al., 2009b). In particular, the decrease in the radial eigenvalues during childhood and increase during adulthood with advancing age may offer early predictors of the regional dynamics of myelination and demyelination (Song et al., 2005).

3.2 Uncinate fasciculus DTI Asymmetry

Our DTI results reproduce an inconsistently reported UF leftward asymmetry of the diffusion tensor anisotropy (Table 1) in healthy children (Eluvathingal et al., 2007) and adults (Kubicki et al., 2002). This trend has not been reported in other studies (Taoka et al., 2006;Lebel et al., 2008; see Table 1) or was even reversed (Rodrigo et al., 2006). A previous postmortem study on the UF cross-sectional area in older adults (Highley et al., 2002; see Table 1), however, reported a rightward asymmetry in UF fiber density, and no age or sex effects.

In our study, the UF diffusion tensor anisotropy leftward asymmetry is more specifically related to a statistically significant leftward asymmetry in the axial diffusivity which could result from a more coherent or less tortuous alignment of fibers (Beaulieu, 2002; Takahashi et al., 2000). Our lifespan cross-sectional study in healthy right-handed controls shows a dissociation between volume-based or macrostructural asymmetry and DTI-based or microstructural asymmetry. Our results on the axial asymmetry should be interpreted carefully as the UF right and left tract volumes were measured using diffusion tensor tractography which is limited by the DTI acquisition spatial resolution and the tracking procedures adopted. The biophysical substrates of this finding require histochemical and postmortem analyses (Beaulieu, 2002; Highley et al., 2002; Takahashi et al., 2000).

3.3 Implications and Significance of the of the Current Study

Our results provide useful baseline data on the effects of side, gender and age on the UF volume and its corresponding DTI metrics. Our results should help in the experimental design of future clinical investigation of the exact functional role of the U.

Access to anatomic information and the pattern of normal developmental trajectory of the uncinate fasciculus expands the breadth and depth of our knowledge of this structure (Schmahamn and Pandya, 2006). The significant role of these patterns of information may play an important role in evaluating fronto-temporal structural and functional connectivity in clinical or psychiatric populations. Since the UF originates from the anterior temporal lobe in front of the temporal horn and the cortical nuclei of amygdala and terminates in several critical areas of the frontal lobes such as orbital frontal cortex. As such the uncinate fasciculus is especially considered to be a critical structure in playing an important role in memory and emotion and our further understanding of these structures may offer new opportunities to provide clinically significant services to patient populations with specific neurologic or psychiatric dysfunctions. An example of such relationship has been recently shown by Fujie et al. (2008). Therefore, our current work on the normal structural development of uncinate fasciculus generates excitement for the expansion of our limited knowledge of brain fiber bundles and their mysterious functional significance.

3.4 Conclusions and Future Plans

Our normative database has been formed by pooling cross-sectional data collected on healthy children and adults using the same DTI protocol (study span ~ 3 years) to help in the interpretation of data collected from patients (Hasan et al., 2008; Hasan et al., 2009b). Our cross-sectional cohort and the lifespan experimental design accounted for the confounding and nonlinear age effects and warrant future longitudinal studies on the structural basis of functional disconnectivity.

Future extensions of the current studies include the investigation in larger samples of males and females of the interplay between UF volume, DTI metrics and the corresponding cortical gray matter thickness and subcortical substrate volume (e.g. hippocampus and amygdala) in both health (Sowell et al., 2003; Walhovd et al., 2005) and disease (Aralasmak et al., 2006; Highley et al., 2002; Kier et al., 2004).

4. Experimental Procedure

4.1 Participants

This study included a total of 108 healthy right-handed children, adolescents and adults (age range 6.7–68.3 years). The cutoff age for children and adolescents was 20 years (Table 2). The boys/girls, men/women and males/females groups were age-matched ($p>0.2$). All participants were primarily English-speaking, identified as neurologically normal by review of medical history, and were healthy at the time of the assessments. The MRI scans were read as “normal” by a board certified radiologist (LAK). Written informed consent from the adults, guardians and adolescents, and assent from the children participating in these studies was obtained per institutional review board regulations for the protection of human subjects.

4.2 MRI and DTI Data Acquisition and Processing

All MRI acquisitions were performed on a 3T Philips Intera scanner with a dual quasar gradient system with a maximum gradient amplitude of 8 Gauss/cm and an eight channel SENSE-compatible head coil(Philips Medical Systems, Best, Netherlands).

The DTI studies utilized a high signal-to-noise ratio (SNR) whole brain DTI protocol that was kept under 7 minutes (Hasan et al., 2007a). The DTI data were acquired using a single-shot spin-echo diffusion sensitized and fat-suppressed echo-planar imaging sequence with the balanced Icosa21 tensor encoding scheme (i.e. twenty-one uniformly-distributed directions over the unit hemisphere) (Hasan, 2007), b-factor = 1000 sec mm^{-2}, repetition time (T_R)/echo time T_E = 7100/65 msec. The echo-planar phase encoding used a SENSE k-space undersampling factor of two (R=2) with an effective k-space matrix of 112×112, image matrix after zero-filling = 256×256. The field-of-view = 240 mm × 240 mm, number of axial sections = 44 with no gap and slice thickness = 3 mm. The number of b~0 magnitude image averages was 6; in addition, each diffusion encoding was repeated twice and magnitude-averaged to enhance the SNR (Hasan, 2007). The SNR, DTI data spatial resolution (e.g. voxel size 2.2 mm × 2.2 mm × 3 mm) and image quality (e.g. reduced image distortions) were adequate to trace the uncinate fasciculus (Eluvathingal et al. 2007; Fujiwara et al., 2008; Hasan et al., 2009a).

In this work, the DTI-derived rotationally-invariant metrics included the fractional anisotropy (FA), axial (L1 = $\lambda_{||}$) and radial diffusivity (LT = $\lambda_{\perp}$). The radial diffusivity is defined as the average of the second and third eigenvalues ($\lambda_{\perp} = (\lambda_2+\lambda_3)/2$) and has been shown by several researchers to be a marker of myelination (Beaulieu, 2002; Song et al., 2005; see also Hasan, 2006). We performed distortion correction to remove eddy-current artifacts, then calculated the ICV from the non-diffusion weighted image (Hasan et al., 2009a). Additional details of DTI image processing (Hasan et al., 2007b; Hasan et al., 2009a) and DTI quality control measures are found elsewhere (Hasan, 2007a).

4.3 Fiber Tracking of the Uncinate Fasciculus

Compact white matter fiber tracking was performed using DTI Studio software (Jiang et al., 2006) based on the fiber assignment by continuous tracking (FACT) algorithm. Diffusion tensor tractography using anatomical landmarks (Kier et al., 2004) and multiple regions-of-interest (ROI) were utilized to trace the UF bilaterally as described elsewhere (Catani et al., 2002; Mori et al., 2002; Jones et al., 2006; Wakana et al., 2007; Yu et al., 2008). The UF tracking used a fractional anisotropy (FA) threshold of 0.15 and angle threshold of 60 degrees. These tracking thresholds were identical to those adopted to trace the UF in two previous publications using the same DTI protocol (Eluvathingal et al., 2007; Hasan et al., 2008). Additional details of the fiber tracking procedures are provided elsewhere (see APPENDIX in Eluvathingal et al., 2007).

In brief, the anterior commissure (AC) identified on a coronal DTI color-coded plane was used as an anatomical landmark to identify the two regions where the UF superior and inferior segments traverse the coronal plane (Figure 3A regions 1 and 2). Note that the seed ROIs selected (Figure 3A) border the external capsule, insula, putamen and the hippocampus (Ebeling and Cramon, 1992). A Boolean "**OR**" operation on region 1 (lower portion of external capsule) combined with an "**AND**" operation on region 2 (temporal lobe) were sufficient to construct the UF on each side avoiding any mixing with other tracts such as the inferior fronto-occipital and inferior longitudinal fascicule (Catani et al. 2002; Mori et al. 2002). Once the UF fiber tract is reconstructed, its volume and corresponding DTI attributes were recorded and visualized in 3D (Figure 3C and 3D).

4.4 Statistical analysis

All analyses of UF absolute, normalized volumes and their corresponding DTI metrics variation were conducted using a generalized linear model with effects of age, side and sex as described elsewhere (Hasan et al., 2007b). Given previous reports on white matter macro and microstructural development across the lifespan (Sowell et al., 2003; Hasan et al., 2007b; Hasan et al., 2009a), both linear and quadratic age terms were included. The DTI metrics (e.g.,

fractional anisotropy = FA; radial or transverse diffusivity = $\lambda_{\perp}$ = LT; axial diffusivity = $\lambda_{||}$ = L1) were modeled for both males and females as $y_f = \beta_0 + \beta_1 * age + \beta_2 * age^2$, and then the general least-squares methods were used to compute the coefficients, standard errors and their significance using analysis-of-variance methods (Hasan et al., 2009a). Interactions of sex with age (both terms) were examined, and trimmed where non-significant. If the quadratic age term was not significant, age and sex interactions were examined without this term, and trimmed if non-significant. All statistical analyses were conducted using SAS 9.1 (SAS Institute Inc, NC) and MATLAB R12.1 Statistical Toolbox v 3.0 (The Mathworks Inc, Natick, MA).

Acknowledgments

This work was funded by NIH-NINDS R01 NS052505-04 awarded to KMH, NIH-NICHD R01 NS046308 awarded to LEC, P01 HD35946 awarded to JMF and 1 P01 NS46588 awarded to ACP. The authors wish to thank Vipul Kumar Patel for helping in data acquisition.

References

1. Antunes NL, Souweidane MM, Lis E, Rosenblum M, Steinherz P. Methotrexate leukoencephalopathy presenting as Klüver-Bucy syndrome and uncinate seizures. Pediatr Neurol 2002;26:305–308. [PubMed: 11992760]
2. Aralasmak A, Ulmer JL, Kocak M, Salvan CV, Hillis AE, Yousem DM. Association, commissural, and projection pathways and their functional deficit reported in literature. J Comput Assist Tomog 2006;30:695–715.
3. Beaulieu C. The basis of anisotropic water diffusion in the nervous system - a technical review. NMR Biomed 2002;15:435–455. [PubMed: 12489094]Review
4. Bendlin BB, Ries ML, Lazar M, Alexander AL, Dempsey RJ, Rowley HA, Sherman JE, Johnson SC. Longitudinal changes in patients with traumatic brain injury assessed with diffusion-tensor and volumetric imaging. Neuroimage 2008;42:503–514. [PubMed: 18556217]
5. Borroni B, Alberici A, Premi E, Archetti S, Garibotto V, Agosti C, Gasparotti R, Di Luca M, Perani D, Padovani A. Brain magnetic resonance imaging structural changes in a pedigree of asymptomatic progranulin mutation carriers. Rejuvenation Res 2008;11:585–595. [PubMed: 18593276]
6. Buckner RL, Head D, Parker J, Fotenos AF, Marcus D, Morris JC, Snyder AZ. A unified approach for morphometric and functional data analysis in young, old, and demented adults using automated atlas-based head size normalization: reliability and validation against manual measurement of total intracranial volume. Neuroimage 2004;23:724–738. [PubMed: 15488422]
7. Burns J, Job D, Bastin ME, Whalley H, Macgillivray T, Johnstone EC, Lawrie SM. Structural disconnectivity in schizophrenia: a diffusion tensor magnetic resonance imaging study. Br J Psychiatry 2003;182:439–443. [PubMed: 12724248]
8. Catani M, Howard RJ, Pajevic S, Jones DK. Virtual in vivo interactive dissection of white matter fasciculi in the human brain. Neuroimage 2002;17:77–94. [PubMed: 12482069]
9. Catani M, Mesulam M. The arcuate fasciculus and the disconnection theme in language and aphasia: History and current state. Cortex 2008;44:953–961. [PubMed: 18614162]
10. Constable RT, Ment LR, Vohr BR, Kesler SR, Fulbright RK, Lacadie C, Delancy S, Katz KH, Schneider KC, Schafer RJ, Makuch RW, Reiss AR. Prematurely born children demonstrate white matter microstructural differences at 12 years of age, relative to term control subjects: an investigation of group and gender effects. Pediatrics 2008;121:306–316. [PubMed: 18245422]
11. Diehl B, Busch RM, Duncan JS, Piao Z, Tkach J, Lüders HO. Abnormalities in diffusion tensor imaging of the uncinate fasciculus relate to reduced memory in temporal lobe epilepsy. Epilepsia 2008;49:1409–1418. [PubMed: 18397294]
12. Dubois J, Hertz-Pannier L, Dehaene-Lambertz G, Cointepas Y, Le Bihan D. Assessment of the early organization and maturation of infants' cerebral white matter fiber bundles: a feasibility study using quantitative diffusion tensor imaging and tractography. Neuroimage 2006;30:1121–1132. [PubMed: 16413790]

13. Duffau H, Gatignol P, Moritz-Gasser S, Mandonnet E. Is the left uncinate fasciculus essential for language?: A cerebral stimulation study. J Neurol. 200910.1007/s00415-009-0053-9

14. Ebeling U, Von Cramon D. Topography of uncinate fascicle and adjacent temporal fiber tracts. Acta Neurochir (Wien) 1992;115:143–148. [PubMed: 1605083]

15. Eluvathingal TJ, Chugani HT, Behen ME, Juhász C, Muzik O, Maqbool M, Chugani DC, Makki M. Abnormal brain connectivity in children after early severe socioemotional deprivation: a diffusion tensor imaging study. Pediatrics 2006;117:2093–2100. [PubMed: 16740852]

16. Eluvathingal TJ, Hasan KM, Kramer L, Fletcher JM, Ewing-Cobbs L. Quantitative diffusion tensor tractography of association and projection fibers in normally developing children and adolescents. Cereb Cortex 2007;17:2760–2768. [PubMed: 17307759]

17. Fujie S, Namiki C, Nishi H, Yamada M, Miyata J, Sakata D, Sawamoto N, Fukuyama H, Hayashi T, Murai T. The role of the uncinate fasciculus in memory and emotional recognition in amnestic mild cognitive impairment. Dement Geriatr Cogn Disord 2008;26:432–439. [PubMed: 18957848]

18. Fujiwara S, Sasaki M, Kanbara Y, Inoue T, Hirooka R, Ogawa A. Feasibility of 1.6-mm isotropic voxel diffusion tensor tractography in depicting limbic fibers. Neuroradiology 2008:131–136. [PubMed: 17938897]

19. Hagmann P, Thiran JP, Jonasson L, Vandergheynst P, Clarke S, Maeder P, Meuli R. DTI mapping of human brain connectivity: statistical fibre tracking and virtual dissection. Neuroimage 2003;19:545–554. [PubMed: 12880786]

20. Hasan KM. Diffusion tensor eigenvalues or both mean diffusivity and fractional anisotropy are required in quantitative clinical diffusion tensor MR reports: fractional anisotropy alone is not sufficient. Radiology 2006;239:611–612. [PubMed: 16641362]

21. Hasan KM. A framework for quality control and parameter optimization in diffusion tensor imaging: theoretical analysis and validation. Magn Reson Imaging 2007a;25:1196–1202. [PubMed: 17442523]

22. Hasan KM, Sankar A, Halphen C, Kramer LA, Brandt ME, Juranek J, Cirino PT, Fletcher JM, Papanicolaou AC, Ewing-Cobbs L. Development and Organization of Human Brain Tissue Compartments across Lifespan using Diffusion Tensor Imaging. Neuroreport 2007b;18:1735–1739. [PubMed: 17921878]

23. Hasan KM, Eluvathingal TJ, Kramer LA, Ewing-Cobbs L, Dennis M, Fletcher JM. White matter microstructural abnormalities in children with spina bifida myelomeningocele and hydrocephalus: a diffusion tensor tractography study of the association pathways. J Magn Reson Imaging 2008;27:700–709. [PubMed: 18302204]

24. Hasan KM, Kamali A, Iftikhar A, Kramer LA, Papanicolaou AC, Fletcher JM, Ewing-Cobbs L. Diffusion tensor tractography quantification of the human corpus callosum fiber pathways across the lifespan. Brain Res 2009a;1249:91–100. [PubMed: 18996095]

25. Hasan, KM.; Kamali, A.; Iftikhar, A.; Datta, S.; Nelson, F.; Wolinsky, JS.; Narayana, PA. Diffusion Tensor Tractogrpahy Quantification of Wallerian Degeneration of the Uncinate Fasciculus in Multiple Sclerosis . Proceedings of the International scoiety for Magnetic Resonance in Medicine (ISMRM) 17th Scientific Meeting & Exhibition; 18–24 April, 2009; Honolulu, Hawai'i, USA. 2009. p. 3196

26. Heiervang E, Behrens TE, Mackay CE, Robson MD, Johansen-Berg H. Between session reproducibility and between subject variability of diffusion MR and tractography measures. Neuroimage 2006;33:867–877. [PubMed: 17000119]

27. Highley JR, Walker MA, Esiri MM, Crow TJ, Harrison PJ. Asymmetry of the uncinate fasciculus: a post-mortem study of normal subjects and patients with schizophrenia. Cereb Cortex 2002;12:1218–1224. [PubMed: 12379610]

28. Houenou J, Wessa M, Douaud G, Leboyer M, Chanraud S, Perrin M, Poupon C, Martinot JL, Paillere-Martinot ML. Increased white matter connectivity in euthymic bipolar patients: diffusion tensor tractography between the subgenual cingulate and the amygdalo-hippocampal complex. Mol Psychiatry 2007;12:1001–1010. [PubMed: 17471288]

29. Jiang H, van Zijl PC, Kim J, Pearlson GD, Mori S. DtiStudio: resource program for diffusion tensor computation and fiber bundle tracking. Comput Methods Programs Biomed 2006;81:106–116. [PubMed: 16413083]

30. Jones DK, Catani M, Pierpaoli C, Reeves SJ, Shergill SS, O'Sullivan M, Golesworthy P, McGuire P, Horsfield MA, Simmons A, Williams SC, Howard RJ. Age effects on diffusion tensor magnetic resonance imaging tractography measures of frontal cortex connections in schizophrenia. Hum Brain Mapp 2006;27:230–238. [PubMed: 16082656]

31. Im K, Lee JM, Lyttelton O, Kim SH, Evans AC, Kim SI. Brain size and cortical structure in the adult human brain. Cereb Cortex 2008;18:2181–2191. [PubMed: 18234686]

32. Kanaan RA, Kim JS, Kaufmann WE, Pearlson GD, Barker GJ, McGuire PK. Diffusion tensor imaging in schizophrenia. Biol Psychiatry 2005;58:921–929. [PubMed: 16043134]Review

33. Kezele IB, Arnold DL, Collins DL. Atrophy in white matter fiber tracts in multiple sclerosis is not dependent on tract length or local white matter lesions. Mult Scler 2008;14:779–785. [PubMed: 18611990]

34. Kier EL, Staib LH, Davis LM, Bronen RA. MR imaging of the temporal stem: anatomic dissection tractography of the uncinate fasciculus, inferior occipitofrontal fasciculus, and Meyer's loop of the optic radiation. AJNR Am J Neuroradiol 2004;25:677–691. [PubMed: 15140705]

35. Kubicki M, Westin CF, Maier SE, Frumin M, Nestor PG, Salisbury DF, Kikinis R, Jolesz FA, McCarley RW, Shenton ME. Uncinate fasciculus findings in schizophrenia: a magnetic resonance diffusion tensor imaging study. Am J Psychiatry 2002;159:813–820. [PubMed: 11986136]

36. Lebel C, Walker L, Leemans A, Phillips L, Beaulieu C. Microstructural maturation of the human brain from childhood to adulthood. Neuroimage 2008;40:1044–1055. [PubMed: 18295509]

37. Levine B, Black SE, Cabeza R, Sinden M, Mcintosh AR, Toth JP, Tulving E, Stuss DT. Episodic memory and the self in a case of isolated retrograde amnesia. Brain 1998;121:1951–1973. [PubMed: 9798749]

38. McDonald CR, Ahmadi ME, Hagler DJ, Tecoma ES, Iragui VJ, Gharapetian L, Dale AM, Halgren E. Diffusion tensor imaging correlates of memory and language impairments in temporal lobe epilepsy. Neurology 2008;71:1869–1876. [PubMed: 18946001]

39. Malykhin N, Concha L, Seres P, Beaulieu C, Coupland NJ. Diffusion tensor imaging tractography and reliability analysis for limbic and paralimbic white matter tracts. Psychiatry Res 2008;164:132–142. [PubMed: 18945599]

40. Mamata H, Mamata Y, Westin CF, Shenton ME, Kikinis R, Jolesz FA, Maier SE. High-resolution line scan diffusion tensor MR imaging of white matter fiber tract anatomy. AJNR Am J Neuroradiol 2002;23:67–75. [PubMed: 11827877]

41. Matsuo K, Mizuno T, Yamada K, Akazawa K, Kasai T, Kondo M, Mori S, Nishimura T, Nakagawa M. Cerebral white matter damage in frontotemporal dementia assessed by diffusion tensor tractography. Neuroradiology 2008;50:605–611. [PubMed: 18379765]

42. Mori S, Kaufmann WE, Davatzikos C, Stieltjes B, Amodei L, Fredericksen K, Pearlson GD, Melhem ER, Solaiyappan M, Raymond GV, Moser HW, van Zijl PC. Imaging cortical association tracts in the human brain using diffusion-tensor-based axonal tracking. Magn Reson Med 2002;47:215–223. [PubMed: 11810663]

43. Nakamura M, McCarley RW, Kubicki M, Dickey CC, Niznikiewicz MA, Voglmaier MM, Seidman LJ, Maier SE, Westin CF, Kikinis R, Shenton ME. Fronto-temporal disconnectivity in schizotypal personality disorder: a diffusion tensor imaging study. Biol Psychiatry 2005;58:468–478. [PubMed: 15978550]

44. Niogi SN, Mukherjee P, Ghajar J, Johnson CE, Kolster R, Lee H, Suh M, Zimmerman RD, Manley GT, McCandliss BD. Structural dissociation of attentional control and memory in adults with and without mild traumatic brain injury. Brain 131:3209–3221. [PubMed: 18952679]

45. Park HJ, Westin CF, Kubicki M, Maier SE, Niznikiewicz M, Baer A, Frumin M, Kikinis R, Jolesz FA, McCarley RW, Shenton ME. White matter hemisphere asymmetries in healthy subjects and in schizophrenia: a diffusion tensor MRI study. Neuroimage 2004;23:213–223. [PubMed: 15325368]

46. Parker GJ, Luzzi S, Alexander DC, Wheeler-Kingshott CA, Ciccarelli O, Lambon, Ralph MA. Lateralization of ventral and dorsal auditory language pathways in the human brain. NeuroImage 2005;24:656–666. [PubMed: 15652301]

47. Price G, Cercignani M, Parker GJ, Altmann DR, Barnes TR, Barker GJ, Joyce EM, Ron MA. White matter tracts in first-episode psychosis: a DTI tractography study of the uncinate fasciculus. Neuroimage 2008;39:949–955. [PubMed: 17988894]

48. Reich DS, Smith SA, Jones CK, Zackowski KM, van Zijl PC, Calabresi PA, Mori S. Quantitative characterization of the corticospinal tract at 3T. AJNR Am J Neuroradiol 2006;27:2168–2178. [PubMed: 17110689]
49. Rodrigo S, Oppenheim C, Chassoux F, Golestani N, Cointepas Y, Poupon C, Semah F, Mangin JF, Le, Bihan D, Meder JF. Uncinate fasciculus fiber tracking in mesial temporal lobe epilepsy. Initial findings Eur Radiol 2007;17:1663–1668.
50. Schmahmann, JD.; Pandya, DN. Fiber Pathways of the Brain. Oxford: New York; 2006.
51. Schmahmann JD, Smith EE, Eichler FS, Filley CM. Cerebral white matter: neuroanatomy, clinical neurology, and neurobehavioral correlates. Ann N Y Acad Sci 2008;1142:266–309. [PubMed: 18990132]
52. Schoene-Bake JC, Faber J, Trautner P, Kaaden S, Tittgemeyer M, Elger CE, Weber B. Widespread affections of large fiber tracts in postoperative temporal lobe epilepsy. Neuroimage. 200910.1016/j.neuroimage.2009.03.013
53. Sheline YI, Price JL, Vaishnavi SN, Mintun MA, Barch DM, Epstein AA, Wilkins CH, Snyder AZ, Couture L, Schechtman K, McKinstry RC. Regional white matter hyperintensity burden in automated segmentation distinguishes late-life depressed subjects from comparison subjects matched for vascular risk factors. Am J Psychiatry 2008;165:524–532. [PubMed: 18281408]
54. Song SK, Yoshino J, Le TQ, Lin SJ, Sun SW, Cross AH, Armstrong RC. Demyelination increases radial diffusivity in corpus callosum of mouse brain. Neuroimage 2005;26:132–140. [PubMed: 15862213]
55. Sowell ER, Peterson BS, Thompson PM, Welcome SE, Henkenius AL, Toga AW. Mapping cortical change across the human life span. Nat Neurosci 2003;6:309–315. [PubMed: 12548289]
56. Szeszko PR, Robinson DG, Ashtari M, Vogel J, Betensky J, Sevy S, Ardekani BA, Lencz T, Malhotra AK, McCormack J, Miller R, Lim KO, Gunduz-Bruce H, Kane JM, Bilder RM. Clinical and neuropsychological correlates of white matter abnormalities in recent onset schizophrenia. Neuropsychopharmacology 2008;33:976–984. [PubMed: 17581532]
57. Takahashi M, Ono J, Harada K, Maeda M, Hackney DB. Diffusional anisotropy in cranial nerves with maturation: quantitative evaluation with diffusion MR imaging in rats. Radiology 2000;216:881–885. [PubMed: 10966726]
58. Taoka T, Iwasaki S, Sakamoto M, Nakagawa H, Fukusumi A, Myochin K, Hirohashi S, Hoshida T, Kichikawa K. iffusion anisotropy and diffusivity of white matter tracts within the temporal stem in Alzheimer disease: evaluation of the “tract of interest” by diffusion tensor tractography. AJNR Am J Neuroradiol 2006;27:1040–1045. [PubMed: 16687540]
59. Wakana S, Caprihan A, Panzenboeck MM, Fallon JH, Perry M, Gollub RL, Hua K, Zhang J, Jiang H, Dubey P, Blitz A, van Zijl P, Mori S. Reproducibility of quantitative tractography methods applied to cerebral white matter. Neuroimage 2007;36:630–644. [PubMed: 17481925]
60. Walhovd KB, Fjell AM, Reinvang I, Lundervold A, Dale AM, Eilertsen DE, Quinn BT, Salat D, Makris N, Fischl B. Effects of age on volumes of cortex, white matter and subcortical structures. Neurobiol Aging 2005;26:1261–1270. [PubMed: 16005549]
61. Wurm G, Wies W, Schnizer M, Trenkler J, Holl K. Advanced surgical approach for selective amygdalohippocampectomy through neuronavigation. Neurosurgery 2000;46:1377–82. [PubMed: 10834642]discussion 1382–1383
62. Yu C, Li J, Liu Y, Qin W, Li Y, Shu N, Jiang T, Li K. White matter tract integrity and intelligence in patients with mental retardation and healthy adults. Neuroimage 2008;40:1533–1541. [PubMed: 18353685]
63. Zahr NM, Rohlfing T, Pfefferbaum A, Sullivan EV. Problem solving, working memory, and motor correlates of association and commissural fiber bundles in normal aging: a quantitative fiber tracking study. Neuroimage 2009;44:1050–1062. [PubMed: 18977450]

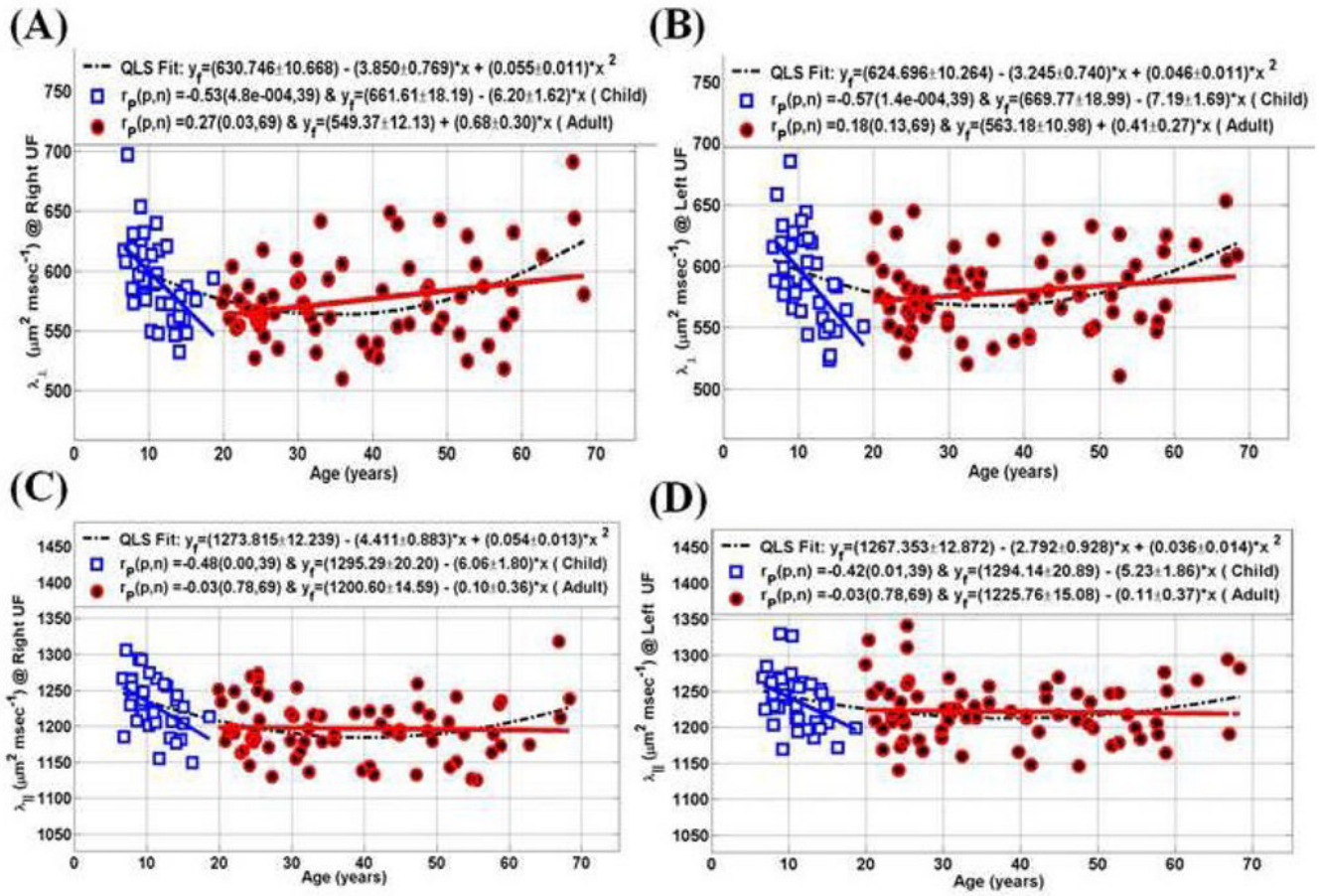

Figure 1.
Graphical summary of the fitted curves (linear and quadratic) of UF on the entire 108 healthy controls ICV normalized UF volume (UFV/ICV ×100%) on the (A) right and (B) left and corresponding fractional anisotropy on the (C) right and (D) left hemispheres.

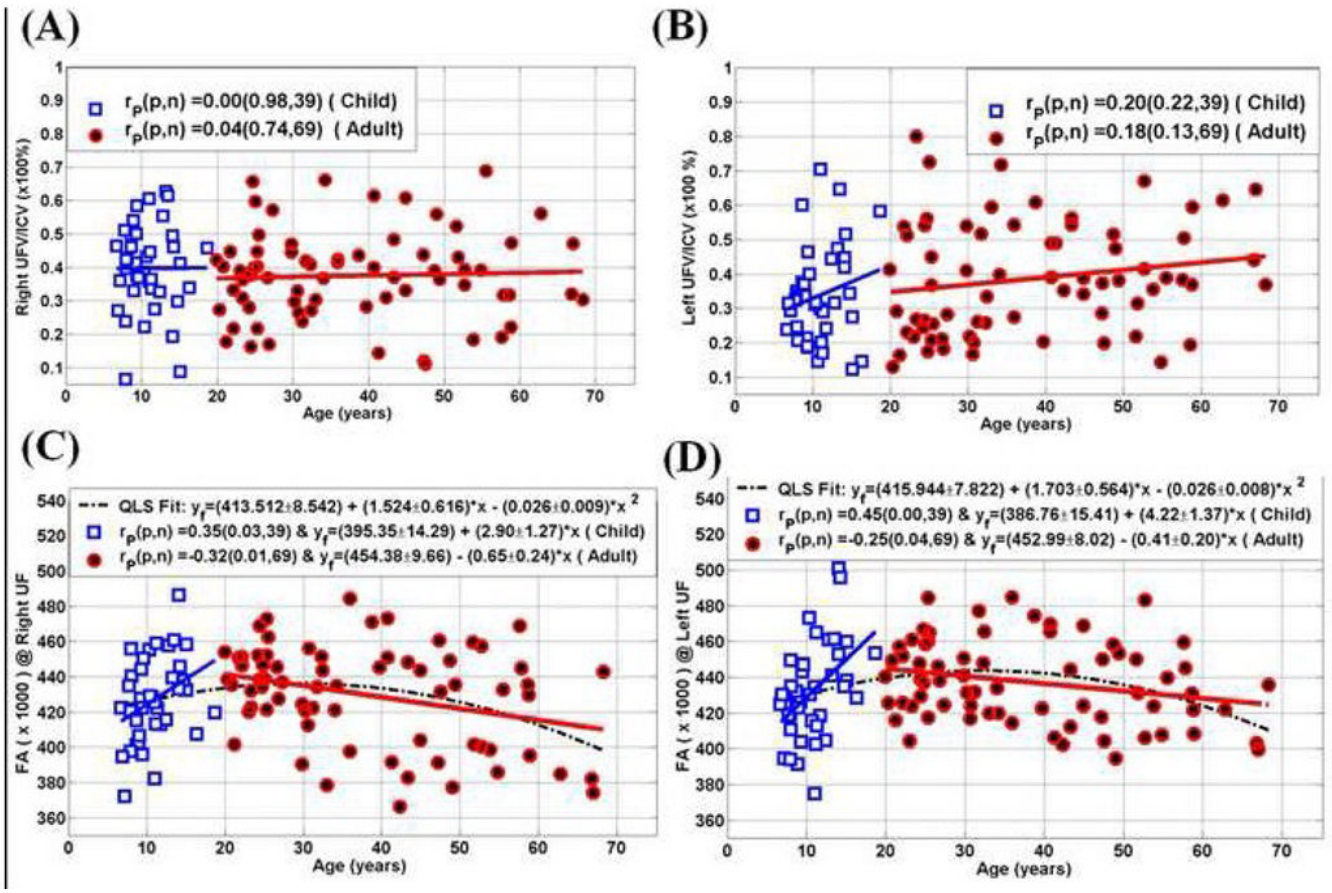

Figure 2.
Graphical summary of the fitted curves of UF on the entire 108 healthy controls of the radial diffusivity on the (A) right and (B) left and axial diffusivity on the (C) right and (D) left hemispheres.

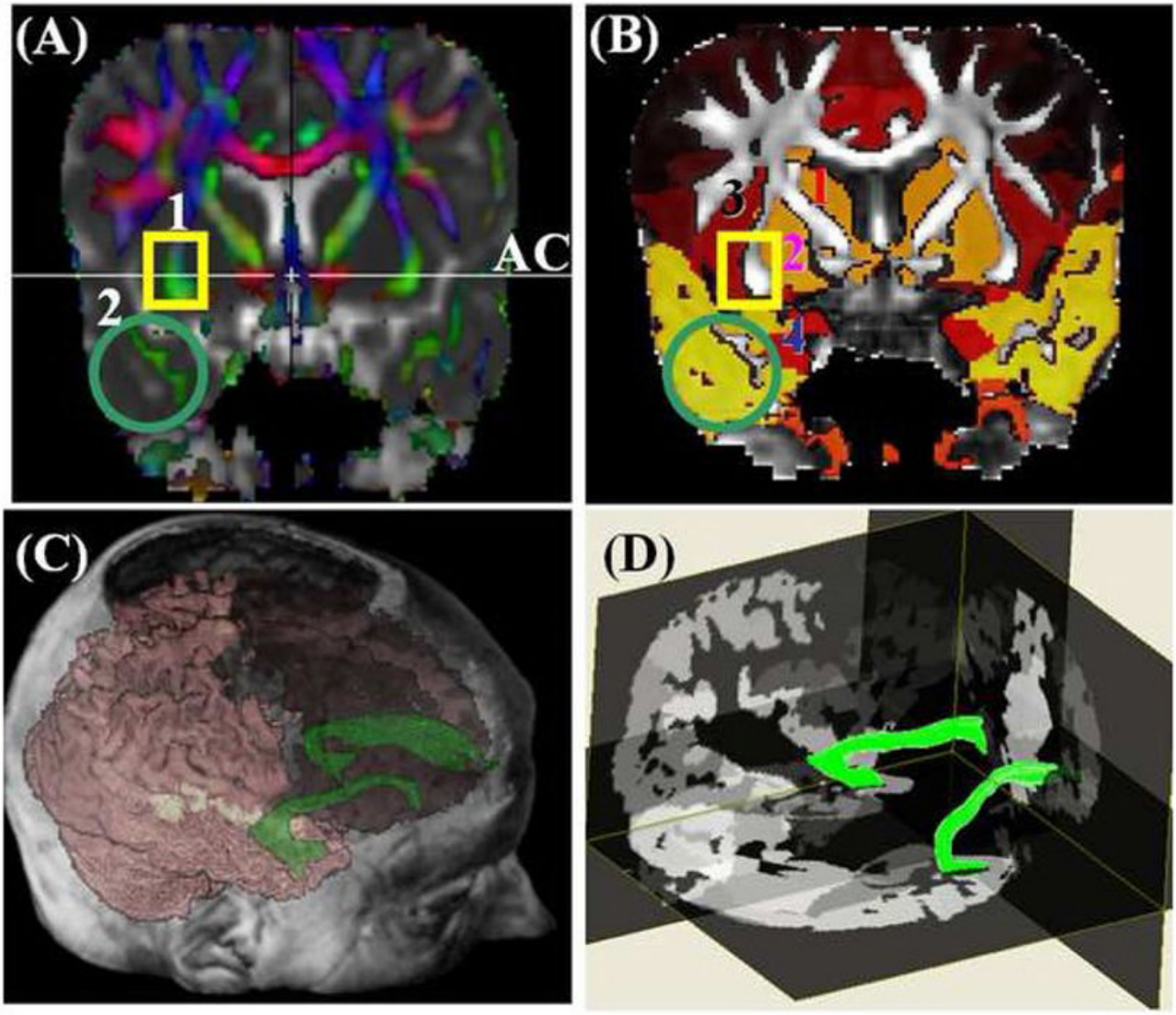

Figure 3.

Illustration of the DTI-based fiber tracking of the uncinate fasciculus (A) The two ROIs (1 rectangle, 2 circle) were placed after identifying the anterior commissure on a coronal DTI color coded map (e.g. principal eigenvector modulated by FA and fused with the mean diffusivity to identify cerebrospinal fluid (CSF) and gray matter) (B) An illustration of the same coronal plane with the two seed ROIs on an FA map showing the gray matter bordering the UF (1 caudate, 2 putamen, 3 insula, 4 amygdala/hippocampus). (C) a 3D postero-lateral view of the right and left UF on a DTI color coded (red = right-left; green = anterior-posterior, blue = inferior superior). Note the origin (temporal lobe) and termination (frontal lobe) of the UF (D) a 3D antero-lateral view of the right and left UF showing the UF position within the cortical and subcortical gray matter structures (e.g. hippocampus).

Table 1

A list of publications that used 10 or more healthy controls that reported some quantitative volumetric and DTI attributes of the uncinate fasciculus.

	Control Demographics			Results and Conclusions
Study	**N(sex/hand) ≥ 10**	**Age**	**Methods**	**Age & Asymmetry**
Dubois et al., 2006	18 (Infants)	12.9 ± 3.4 wks	DT-FT&ROI	p(D_{av}, age) = 0.001; FA(age) = n.s.
Eluvathingal et al., 2007	29 (13Boys/16Girls)	10.7 ± 2.9 yrs	DT-FT	FA (Left > Right); r(FA, age) > 0.4; p<0.03
Highley et al., 2002	11 Women 10 Men	74.5 ± 12.5 yrs 70.0 ± 14.1 yrs	Postmortem Histology	Area, axons # and density Right > Left (rightward asymmetry) No age, sex effects
Jones et al., 2006	14 Rh (Adults)	19–57 yrs	DT-VBA	R (FA, age) = −0.53 (p=0.049)
Kubicki et al., 2002	18 Rh (Adults)	43± 6 yrs	DT-ROI	FA (Left > Right) Area (Left > Right)
Lebel et al., 2008	202 (98 Females; 187 Rh)	15.2 ± 6.1 yrs 5.6–29.2 yrs	DT-FT	r (FA, age) = 0.514 Minimal sex and asymmetry effects
Malykhin et al., 2009	24 (6 Men)	32 ± 8 yrs	DT-FT	FA (Left ~ Right) UFV Right = 1.108 mL UFV Left = 0.802
Nakamura et al., 2007	15 (Men)	32.7 ± 12.4 yrs	DT-ROI	FA (Left UFV ~= Right UFV) Left UF-area (22.0 ± 6.8 mm^2) Right UF-area (21.8 ± 7.4 mm^2)
Park et al., 2004	32 (Men)	44 ± 5.6 yrs	DT-VBA	FA (Left > Right) superior portion FA (Right > Left) inferior portion
Rodrigo et al., 2006	10 (6 Men) Rh	20–33 yrs	DT-FT	FA (Right > Left)
Taoka et al., 2006	15 (11Women)	~ 72 ± 3 yrs	DT-FT	FA (Right ~= Left) Right UFV = 0.475 ± 0.211 mL Left UFV = 0.502 ± 0.216 mL
Wakana et al., 2007	10 (5 Men)	26.1 ± 5.48 yrs	DT-FT	Left UFV (~ 3 ± 2 mL) Right UFV (~ 1.5 ± 1) Volume (Left > Right; p < 0.05) FA (Right ~= Left)

Abbreviations used in Table 1

D_{av} = Mean diffusivity; FA = fractional anisotropy; n. s. = not significant

Rh = Right-handed

DT-FT = diffusion tensor fiber tracking; DT-ROI = diffusion tensor region-of-interest; DT-VBA = diffusion tensor voxel based anisotropy

UFV = uncinate fasciculus volume in mL = cm^3

~ = approximately equal to or not statistically different

Table 2

The mean values (MN) and standard deviations (± SD) of the (a) intracranial volume (mL = cm^3) and diffusion tensor tracking-based (b) absolute (c) ICV-normalized volume (UFV/ICV × 100%) of all possible subgroups in our cohort along with the *P* values comparing the results between boys/girls, men/women and males/females.

ICV, Volumetry RUFV/ICV (×100%) LUFV/ICV (×100%)	**ICV MN ± SD (mL)**	**RUFV MN ± SD (mL)**	**LUFV MN ± SD (mL)**	**RUFV/ICV (×100)**	**LUFV/ICV (×100)**
Boys	1547.0±99.0	6.43±2.24	4.96±2.08	0.414±0.134	0.319±0.124
Girls	1434.1±114.6	5.40±1.82	5.17±2.35	0.377±0.129	0.361±0.158
Children	1494.9±119.5	5.96±2.11	5.06±2.19	0.398±0.132	0.338±0.140
P(Boys vs. Girls)	0.002	0.13	0.78	0.40	0.37
Men	1504.3±150.4	5.96±1.95	5.41±2.29	0.396±0.121	0.364±0.161
Women	1378.5±107.4	4.96±1.87	5.48±2.19	0.361±0.140	0.401±0.163
Adults	1425.9±138.6	5.33±1.95	5.46±2.21	0.374±0.134	0.388±0.163
P(Men vs. Women)	0.0001	0.04	0.88	0.34	0.37
Males	1523.4±130.4	6.17±2.08	5.22±2.19	0.403±0.127	0.343±0.145
Females	1394.9±111.6	5.09±1.85	5.41±2.21	0.367±0.137	0.388±0.161
All	1450.8±135.6	5.56±2.00	5.33±2.19	0.382±0.132	0.369±0.156
P(Males vs. Females)	2.5×10^{-7}	0.0056	0.66	0.16	0.14

Abbreviations for Tables 2-5

ICV = intracranial volume

MN = mean values, SD standard deviations

RUFV, LUFV = right/left uncinate fasciculus volume

FA = fractional anisotropy

LT = radial diffusivity ($\lambda_\perp$)

L1 = axial diffusivity ($\lambda_\parallel$)

Table 3

The mean values and standard deviations of FA, radial and axial diffusivities of all possible subgroups in our cohort along with the *P* values comparing the results between boys/girls, men/women and males/females.

	FA(RUFV) MN ± SD (×1000)	FA(LUFV) MN ± SD (×1000)	LT(RUFV) MN ± SD (m^2/msec)	LT(LUFV) MN ± SD (m^2/msec)	L1(RUFV) MN ± SD (m^2/msec)	L1(LUFV) MN ± SD (m^2/msec)
Boys	427.2±27.1	431.2±29.2	593.3±41.0	594.5±40.6	1227.7±41.7	1239.6±40.1
Girls	426.5±20.5	434.4±25.2	595.4±23.7	588.3±31.6	1231.5±29.8	1234.6±31.9
Children	426.8±24.0	432.7±27.1	594.3±33.8	591.6±36.4	1229.4±36.3	1237.3±36.1
P (Boys vs. Girls)	0.93	0.72	0.85	0.60	0.75	0.67
Men	433.1±28.9	436.5±23.5	571.2±32.4	583.4±32.6	1196.1±42.8	1229.3±41.4
Women	427.4±28.2	437.6±23.0	578.2±36.7	576.3±30.3	1197.3±39.9	1217.1±42.2
Adults	429.5±28.4	437.1±23.1	575.5±35.1	579.1±31.1	1196.8±40.7	1221.7±42.1
P (Men vs. Women)	0.43	0.85	0.43	0.36	0.91	0.25
Males	430.4±27.9	434.1±26.0	581.1±37.8	588.4±36.4	1210.2±44.7	1233.9±40.7
Females	427.1±26.0	436.6±23.5	583.2±34.2	579.8±30.9	1207.4±40.1	1222.3±40.0
All	428.6±26.8	435.5±24.6	582.3±35.6	583.6±33.5	1208.6±42.0	1227.3±40.0
P (Males vs. Females)	0.53	0.60	0.76	0.19	0.73	0.14

Abbreviations for Tables 2-5

ICV = intracranial volume

MN = mean values, SD standard deviations

RUFV, LUFV = right, left uncinate fasciculus volume

FA = fractional anisotropy LT = radial diffusivity ($\lambda_\perp$)

L1 = axial diffusivity ($\lambda_\parallel$)

Table 4

The Pearson correlation coefficient and significance of the linear regression fit model in both children and adults for the UFV/ICV, FA, radial and axial diffusivities. The linear regression curves are shown in Figure 2 and Figure 3.

Pearson Correlation Coefficients of age vs. UF volumetry and DTI metrics	Children r(p)	Adults r(p)
UFV (Right)/ICV vs. age	0.00 (0.98)	0.04 (0.74)
UFV (Left)/ICV vs. age	0.20 (0.22)	0.18 (0.13)
FA (Right) vs. age	0.35 (0.03)	−0.32 (0.01)
FA (Left) vs. age	0.45 (< 0.0001)	−0.25 (0.04)
LT (Right) vs. age	−0.53 (< 0.0005)	0.27 (0.03)
LT (Left) vs. age	−0.57 (< 0.0002)	0.18 (0.13)
L1 (Right) vs. age	−0.48 (< 0.0001)	−0.03 (0.78)
L1 (Left) vs. age	−0.42 (0.01)	−0.03 (0.78)

Abbreviations for Tables 2-5

ICV = intracranial volume

MN = mean values, SD standard deviations

RUFV, LUFV = right/left uncinate fasciculus volume

FA = fractional anisotropy

LT = radial diffusivity ($\lambda_{\perp}$)

L1 = axial diffusivity ($\lambda_{\parallel}$)

Table 5

Diffusion tensor fiber tracking-based estimation of the FA, radial and axial diffusivities corresponding to the right and left UF fit statistics in all controls.

Diffusion Tensor Metrics of the Uncinate Fasciculus	Quadratic Fit Model: $y=\beta_0+\beta_1^{*}\,age+\beta_2^{*}\,age^2$			
	R^2	β_0±SD (p)	β_1±SD (p)	β_2±SD (p)
FA (× 1000)	0.084	413.512±8.542	1.524±0.616	−0.026±0.009
Right		(p*)	(0.015)	(0.005)
FA (× 1000)	0.087	415.944±7.822	1.703±0.564	−0.026±0.008
Left		(p*)	(0.003)	(0.002)
LT(μm²/msec)	0.193	630.746±10.668	−3.850±0.769	0.055±0.011
Right		(p*)	(p*)	(p*)
LT (μm²/msec)	0.155	624.696±10.264	−3.245±0.740	0.046±0.011
Left		(p*)	(p*)	(p*)
L1 (μm²/msec)	0.236	1273.815±12.239	−4.411±0.883	0.054±0.013
Right		(p*)	(p*)	(p*)
L1 (μm²/msec)	0.093	1267.353±12.872	−2.792±0.928	0.036±0.014
Left		(p*)	(0.003)	(0.010)

*P<0.00001

Abbreviations for Tables 2-5

ICV = intracranial volume

MN = mean values, SD standard deviations

RUFV, LUFV = right/left uncinate fasciculus volume

FA = fractional anisotropy

LT = radial diffusivity ($\lambda_{\perp}$)

L1 = axial diffusivity ($\lambda_{\|}$)

Table 6

Basic demographics of the healthy control population in the current study.

Gender and Age Distribution and Demographics	N	Age range (years)	Age Mean ± SD (years)
Boys	21	6.67 – 16.33	11.23 ± 2.89
Girls	18	6.92 – 18.67	10.44 ± 2.94
Children	39	6.67 –18.67	10.87 ± 2.90
P(Boys vs. Girls)			0.40
Men	26	19.9 – 68.3	38.11±14.22
Women	43	20.3 – 67	38.29±13.75
Adults	69	19.9 – 68.3	38.22±13.83
P(Men vs. Women)			0.96
Males	47	6.7 – 68.3	26.10±17.20
Females	61	6.92 – 67	30.07±17.29
All	108	6.67 – 68.3	28.35±17.28
P(Males vs. Females)			0.24